

Amino functionalized mesoporous silica for drug adsorption

N. Benyoub^{*1}, A. Benhamou¹, A. Debab¹

¹Laboratory of Process Engineering and Environment, University of Sciences and Technology of Oran Mohamed Boudiaf USTO-MB-, Faculty of chemistry, BP 1505 El-Mnouar, Oran-ALGERIA

*Corresponding author: nassima.benyoub@univ-usto.dz ; Tel.: +213 775 997 759

ARTICLE INFO

Article History:

Received : 29/01/2020
Accepted : 28/02/2021

Key Words:

MCM-41;
Functionalization;
Adsorption;
Pharmaceutical residues;
Wastewater treatments.

ABSTRACT/RESUME

Abstract: The main objective of this work was to synthesize hexagonal mesoporous materials such as MCM-41 from optimized protocols and to test their effectiveness in adsorption of different pharmaceutical pollutants. First, pore size and the specific surface area of the base materials have been modified by incorporation of amino groups in post-synthesis, by selective extraction of the loaded groups and finally by calcination. Subsequently, adsorbent products were characterized by their mesoscopic textures, structures and controls using different methods: X-Ray Diffraction (XRD), Specific Surface Area (BET), Fourier Transform Infrared Spectroscopy (FTIR), Thermogravimetric analyses (TGA/DTA) and Zetametry. Finally, their adsorption capacities were evaluated using several pharmaceutical residues under standard conditions (such as Diclofenac, Cefalexin ...). The results obtained during the adsorption study showed the effectiveness of these materials for the decontamination of aqueous media contaminated with pharmaceutical residues. Kinetic and adsorption isotherm studies were carried out to clarify the method of binding of the selected pharmaceutical pollutants to the tested materials.

I .Introduction

Over the last twenty years, the chemistry of inorganic nanostructured materials has been greatly expanded with the advent of soft "sol-gel" chemistry [1]. Thus, in the early 1990s, Mobil scientists proposed the first syntheses of mesostructured silicates, ie materials with an organized porous system consisting of mesopores [2-4] Since then, many research groups have patented new families of materials with different structures, pore sizes and modes of synthesis: several methods are needed in the way of manufacturing new organized porous materials "MPO" [5].

Since, a new family of ordered mesoporous solids is widely studied by many researchers from different horizons for various applications including adsorption and catalysis. In the field of catalysis, many studies report information on different methods of synthesis, and characterization, so a

wide variety of catalysts based on different mesoporous materials has been implemented and used in different types of catalysis (acidic, basic, chiral) [6].

In the field of adsorption, specifically in an aqueous medium, various mesoporous materials such as: MCM-41, MSU, SBA-15, SBA-16, have been functionalized by various groups for the adsorption of metal ions and various organic pollutants. (pharmaceutical substances) [7-13].

Pharmaceutical substances are active molecules used to induce a favorable effect on health in the animal or human organism (diagnosis, treatment of diseases, etc) [14]. Their large use is therefore at the origin of widespread contamination of aquatic environments by a variety of molecules [15]. It was reported for the first time in the United States in the 1970s following the detection of antibiotics in wastewater [16]. Ten years later, drug residues were detected in Britain. Nevertheless, it was only from

the 1990s that knowledge about this environmental contamination developed. Pharmaceuticals can be considered as persistent and harmful micropollutants because of their continuous release into the environment and sometimes their intrinsic properties (toxic, metabolic, hardly biodegradable etc) [14, 17].

Indeed, studies and analysis techniques have allowed the detection of quantities of the order of $\mu\text{g} / \text{l}$ in samples of domestic wastewater and water intended for consumption [13-27]. The contamination of aquatic environments (surface water and those intended for consumption) by pharmaceutical residues has therefore been the subject of increasing studies over the past ten years [13, 15, 17, 28].

The main objective of this work is to synthesize MCM-41 hexagonal mesoporous material, to modify it by: the addition of organic groups, the selective extraction and the calcination, then to evaluate the adsorption capacity of prepared materials on different pharmaceutical pollutants. A kinetic study and that of adsorption isotherms will also be discussed.

II .Synthesis and Characterization

II.1. Materials and reagents

Cetyltrimethylammonium Bromide 99% (CTAB); Smoked Silica (SiO_2) 98%; Tetramethylammonium Hydroxide (TMAOH); Tetraethylorthosilicate 99% (TEOS); N-N, Dimethyl-dodecylamine (DMDDA) 98% ; Ethanol 96%.

II.2. Synthesis methods

MCM-41 Synthesis

The pure silica MCM-41 was prepared according to an optimized protocol [29]. The synthetic gel is initially heated to 100°C for 2 days. TMAOH and CTAB were added to the distilled water under stirring until the solution became clear. The silica source was added to the stirred solution for 2 h. The gel was transverse in a Teflon-coated autoclave, then sealed and placed in the oven at 100°C for 48 h. The product was recovered by vacuum filtration and washed several times with distilled water, then dried at 100°C to obtain a white powder at the end, which is called "MCM-41/P" parent material.

Functionalization of materials

An amount of MCM-41/P is added to an emulsion consisting of water and NN-Dimethyl-dodecylamine (DMDDA) stirred previously for 5 min. This mixture is left under agitation for 30 min, then transferred to a Teflon reactor and placed in an oven set at 120°C for 3 days. The resulting material is filtered and washed several times with distilled water and then dried at room temperature (20°C): it is the amino material "DMDDA-41/A" [29].

Other modifications can also be made: the material MCM-41/P is calcined directly at 550°C for 7 hours, resulting in a parent/calcined material "MCM-41-P/C". Then, the selective extraction of the amine DMDDA is done using a specific solvent which is ethanol using a soxhlet gives us the deaminated material "DMDDA-41/B". And at the end, the calcination of the material A and/or B at 550°C for 7 h at a heating rate of $1^\circ\text{C}/\text{min}$ gives the calcined material "DMDDA-41/C".

II.3. Characterization techniques

This characterization aims in a very detailed way, the study and identification of the textural, structural and surface properties, as well as the electrochemical properties of the surface of the materials obtained. A combination of physico-chemical (X-ray diffraction, BET, ATG/ATD and Zetametry) and spectroscopic (FTIR) techniques is performed and their understanding could allow a good exploitation of these materials for specific applications.

III .Results and discussions

III.1. Characterization

Low angle X-ray diffraction is used to demonstrate the arrangement of channels created by surfactant micelles.

Fig 1 shows the diffractograms measured from 0.5 to 6 degrees (2θ) of the materials DMDDA-41/A, DMDDA-41/B and DMDDA-41/C. These three materials are compared to MCM-41/P-C which is the base material. For each of the materials, there is a very intense main peak of about 2.2° [hkl plane (100)] followed by three other low intensity peaks. These peaks are similar and characterize a preserved and well-ordered mesoporous structure with a hexagonal symmetry of pores P6 mm [2, 4, 30].

Maximum slip (MCM-41/P-C and DMDDA-41/B) is observed at higher diffraction angles [23, 31] resulting in smaller interplanar distances as shown in Table 1.

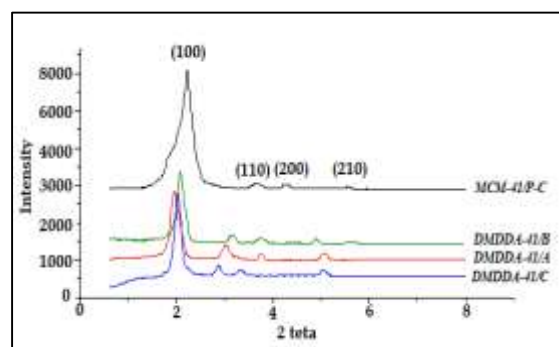


Figure 1. Diffractograms of materials (parent, amino, deaminated and calcined)

The adsorption-desorption isotherms of the parent MCM-41 and these modified forms are illustrated in Fig 2. This is type IV according to the IUPAC classification and hysteresis H1 which is representative of structured mesopores [32- 33].

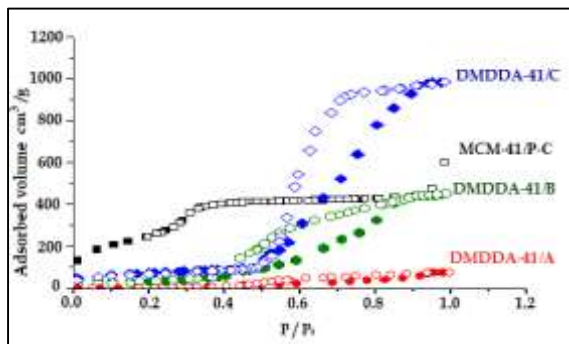


Figure 2. Isotherm of adsorption / desorption of Si-MCM-41 materials

For MCM-41/P-C, there is an increasing slope for low relative pressures $0 < (P/P_0) < 0.3$ corresponding to a single-layer filling of the surface [29, 34-35], followed by a steep slope of the curve for relative pressures between $0.3 < (P/P_0) < 0.8$, due to capillary nitrogen condensation into mesopores. And towards $(P/P_0) > 0.8$ there is a multilayer adsorption on the surface of the base material.

For the material DMDDA-41/A, at relative pressures $(P/P_0) < 0.4$, a single layer filling of the surface is obtained and for $(P/P_0) > 0.5$ a multilayer adsorption plateau appears. The same observations as for the original material are noted for DMDDA-41/B and DMDDA-41/C. For the last two, the relative low pressure plate is almost identical ($(P/P_0) < 0.5$), but the distinction is in the slopes of the following plate: steep slope towards the calcined material (up to 1 in (P/P_0)) unlike the deaminated material ($0.5 < (P/P_0) < 0.8$).

In the case of these two materials, the desorption does not follow the adsorption creating an H1 type hysteresis which closes abruptly at $(P/P_0) = 0.5$ for DMDDA-41/C and at $(P/P_0) = 0.4$ for DMDDA-41/B, this suggests a capillary condensation phenomenon in mesopores. The width of the hysteresis increases (DMDDA-41/C) indicating that the pore size distribution is much wider in the calcined material (Fig 3) [29, 36-38].

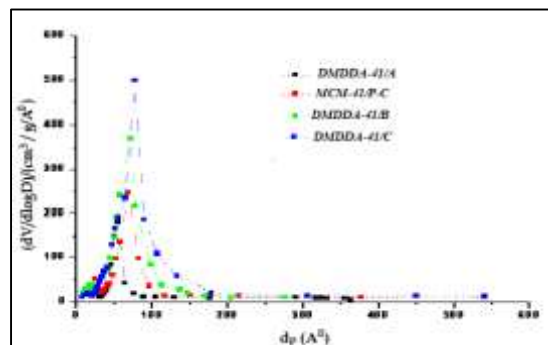


Figure 3. Distribution of pore diameters of materials MCM-41

The pore diameter distributions shown in Fig 3 show that the prepared materials have different pore diameters. The traces are all centered, indicating a better uniformity of pore diameter. The widening of the pore diameter distribution indicates the formation of a less homogeneous pore network.

The analysis of these data shows large differences in the parameters of the four materials. The results of pore surface area, diameter and volume decrease remarkably for amino material (the surface area and part of the pore volume are occupied by amines), unlike MCM-41/P-C. Then, the deamination increases these parameters again, while the calcination leads to higher values (see Table 1).

The FTIR spectra of the prepared MCM-41 materials are shown in Fig 4 where some vibration bands are present in the materials: they are similar to those of amorphous silica.

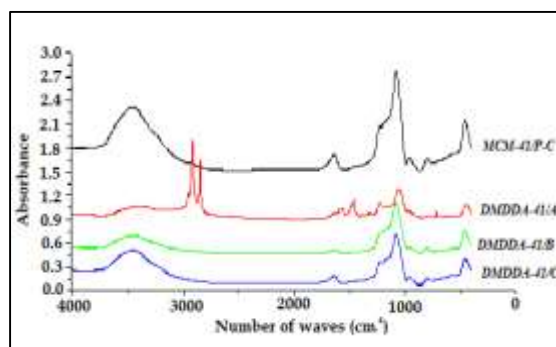


Figure 4. IRTF Spectrum of Si-MCM-41

The wide band between 3450 cm^{-1} , characteristic of the elongation of the bond (O-H), water and silanol groups on the surface. Another vibrating band (O-H) noted around 1650 cm^{-1} indicates the presence of water in the materials. At 1100 cm^{-1} , an asymmetric elongation junction (O-Si-O) of the tetrahedral entities SiO_4 was observed, while about 950 and 750 cm^{-1} , two bends characteristic of the asymmetric elongation of the bond (Si-O) of the same entities present. We also note the presence of

a band characterizing the deformation of the angle (O-Si-O) of the tetrahedral entities SiO₄, this around 450cm⁻¹ [29, 35, 39, 40].

In addition to these bands, the amino material (DMDDA-41/A) records two new bands characteristic of the amino groups: the first located at 2900 cm⁻¹ characterizes the vibrations (CN), while the second one is observed at 1480 cm⁻¹ resulting from the deformation vibration of the bonds (NH) [36, 41, 42].

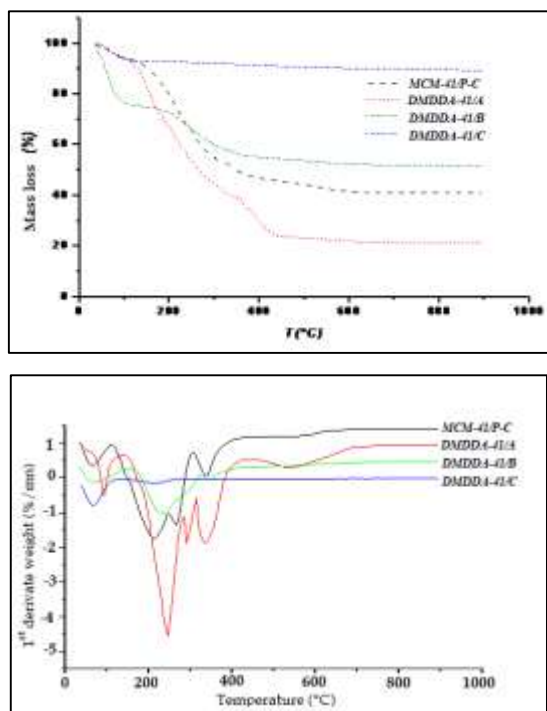


Figure 5. Thermogravimetric Analysis A- (TGA) & Differential Thermal Analysis B-(DTA) of the different materials

The TAG /DTA thermogravimetric analysis of all the materials is represented by two Figs 5A and 5B, from which there are three different zones of mass variation as a function of temperature [30].

The 1st zone at low temperature (25<T <160°C.) corresponds to dehydration of the water physisorbed on the surface of the material. The 2nd intermediate zone (160<T<600°C) corresponds to the decomposition and volatilization of the organic compounds (surfactants and amine) in strong interaction with the surface of the material (covalent and electrostatic bonds).

The last high temperature zone (600<T<900°C): assigned to silica dehydroxylation phenomena

(condensation of the remaining silanols causing the elimination of water molecules) [3, 29, 34, 43].

Fig 6 shows the zeta potential curves $\zeta = f(\text{pH})$ of the different MCM-41 materials in the range of pH 2 to 11. Each point $\zeta = f(\text{pH})$ is the average of the results obtained on electrophoretic mobility measurements from 100 to 500 p at a zeta potential between 5 and 8 mV. The pH for which the zeta potential is zero (no movement of particles under the effect of the electric field) is called the isoelectric point (IPE).

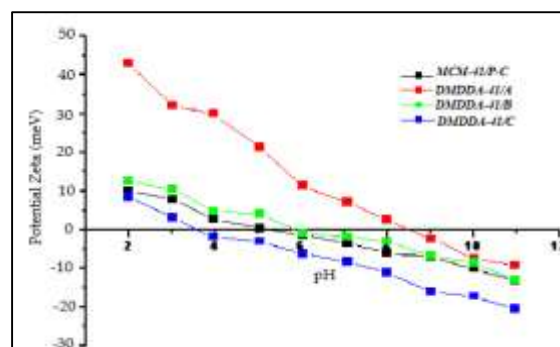


Figure 6. Zeta potential of MCM-41 materials modified by DMDDA

The parent material MCM-41/P has positive potentials between 2 <pH<5 and negative potentials from pH=5.5. For DMDDA-41/A, it has positive potentials between 2 <pH <8.5 and negative potentials from pH=8.5. Then, DMDDA-41/B has positive potentials between 2 <pH <6 and negative potentials from pH=6.1. And for the calcined material DMDDA-41/C, it has positive potentials between 2 <pH <3.6 and negative potentials from pH=3.6 [19, 36].

All the data from the characterization of the different prepared materials are grouped in Table 1.

Table 1. Characterization Data of Si- MCM-41 Materials

Materials	X-Ray diffraction			BET (at 77°K)			TGA/DTA (Mass loss %)			Zetametry
	2 θ (°)	d ₁₀₀ (nm)	a ₀ (nm)	S _{BET} (m ² /g)	d _p (nm)	V _p (cm ³ /g)	1 st Zone	2 nd Zone	3 rd Zone	PIE (isoelectric point)
DMDDA-41/C	2.02	4.48	5.17	1246	10.6	1.86	7.02	2.76	0.87	3.6
DMDDA-41/B	2.10	4.21	4.86	387	5.84	1.07	15.67	45.97	1.63	5.8
DMDDA-41/A	1.97	4.39	5.07	74	-	0.28	3.51	70.67	3.59	8.7
MCM-41/P-C	2.28	3.87	4.47	1147	3.22	0.85	8.23	48.41	1.43	5.6

III.2. Adsorption study

Different adsorption tests were performed on three (03) active ingredients selected as pollutants for the different mesoporous materials MCM-41, calcined MCM-41, functionalized MCM-41 (DMDDA), deaminated MCM-41 and functionalized calcined MCM-41(DMDDA). Under magnetic stirring, each material is added to 20 ml of drug solution at a diluted concentration, then after filtration through a filter of 0.45 μm , the filtrates are analyzed by UV-Visible spectrophotometry to measure absorbance at $\lambda_{\text{max}} = 236, 262$ and 276 nm for Prednisolone, Cefalexin and Diclofenac respectively.

It should be noted that the functionalized and then deaminated form DMDDA-41/A has the greatest binding capacity with respect to Prednisolone and Cefalexin, followed by DMDDA-41/A (amino form) then MCM-41/P (parent form) and finally the two calcined forms of MCM-41.

In the case of Diclofenac, the amino form DMDDA-41/A has the highest adsorption affinity, followed by the deaminated material, then the parent and lastly the calcined forms. These variations are due to the physico-chemical properties of the materials in terms of specific surfaces, porosity and most importantly the surface load as a function of existing groups (the amino material DMDDA-41/A is loaded with NH_2 compared to DMDDA-41/B).

Fig 7 illustrates the kinetics study of the four pollutants selected on the DMDDA-41/B (the material that presented the maximum retention capacity). This study is necessary to predict the equilibrium time that will be taken into account for further work. According to the figure, the appearance of the curves presents two areas:

- From 0 to 50 min: zone that reveals rapid adsorption and occurs at accessible sites on the surface.
- From 50 to 120 min: the adsorbed quantities evolve more slowly, due to the diffusion inside the pores of the material, until reaching a plateau

corresponding to the equilibrium at the end of 120 minutes [22, 26, 44-48].

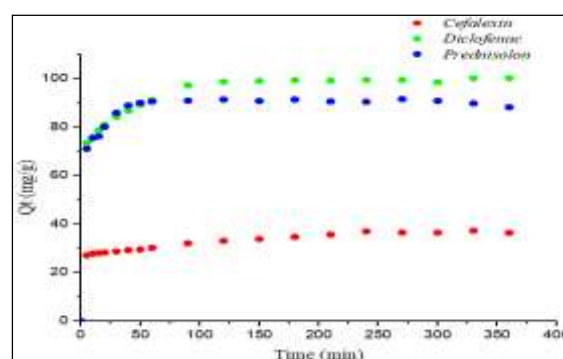


Figure 7. Kinetics of elimination of active ingredients on DMDDA-41/B

The same findings were noted for the amino material DMDDA-41/A. It is also noted that there are no major differences between the two materials (the nature and especially the charge of their specific surfaces allow them to have an almost typical attractive behaviour towards the chosen active ingredients).

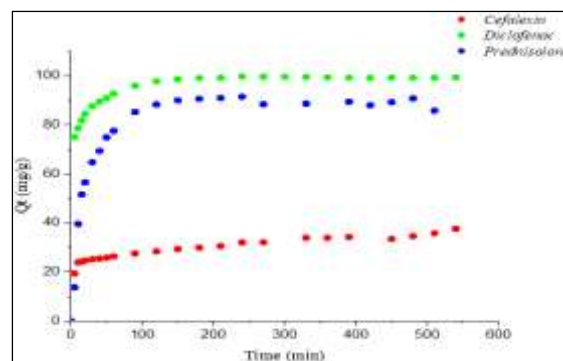


Figure 8. Kinetics of elimination of active ingredients on DMDDA-41/A

The adsorption process is best described by studying first- and second-order pseudo-kinetic models. For pseudo-first order process, the Lagergren rate equation is the one generally used:

$$\ln(Q_e - Q_t) = \ln Q_e - k_1 t \quad (1)$$

Where Q_e is the equilibrium adsorption amount, Q_t the adsorption amount at time t and k_1 is the pseudo-first order rate constant.

The pseudo-second order process can be expressed as the equation:

$$\left(\frac{t}{Q_t}\right) = \left[\frac{1}{k_2 \times Q_e^2}\right] + \left[\frac{1}{Q_e}\right] \quad (2)$$

Where Q_e is the equilibrium adsorption amount, Q_t the adsorption amount at time t and k_2 is the pseudo-second order rate constant.

Figs 9A and 9B and Figs 10A and 10B represents the linearization of the two kinetic models for pharmaceutical pollutants and the parameter values of the two kinetic models applied to their removal are grouped in Table 2.

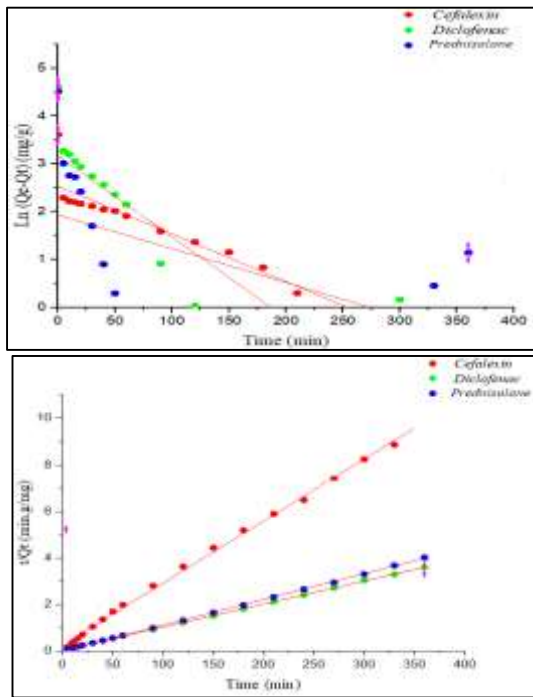


Figure 9. Application of the pseudo-first order (A) and pseudo-second order (B) model to the elimination of active ingredients on MCM-41/DMDDA-B

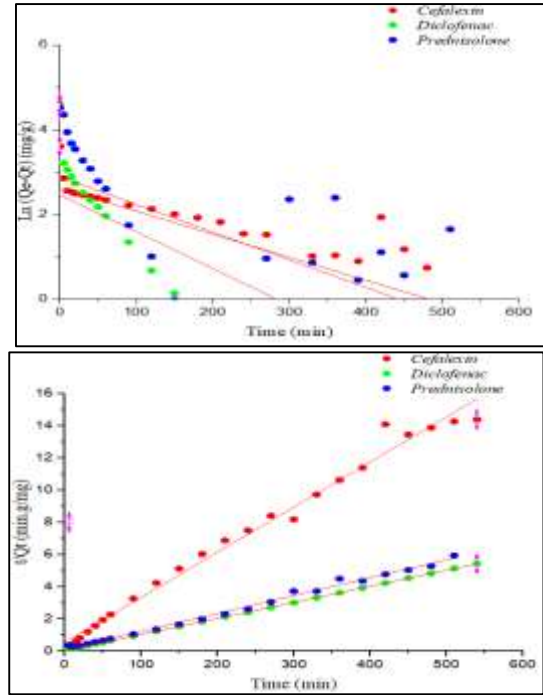


Figure 10. Application of the pseudo-first order (A) and pseudo-second order (B) model to the elimination of active ingredients on MCM-41/DMDDA-A

According to the kinetic constant values, the kinetics of pharmaceutical pollutants follow the pseudo second order model ($R^2 \approx 0.99$), rather than the pseudo first one.

Batch solutions of the selected active ingredients were prepared separately and then tested, each with the deaminated material DMDDA-41/B and then the amino material DMDDA-41/A. These tests are performed to determine the amount of adsorption achieved according to the modifications made and to describe the adsorption process in heterogeneous systems. The results obtained can be adjusted by different isothermal equations, including those worked with: the Langmuir model, Freundlich and Sips [32].

Langmuir assumes that adsorption is done in a monolayer on the surface of the solid, Freundlich's considers that there are different types of adsorption sites distributed when at Sips, it is an isotherm that allows to simulate both the Langmuir model and Freundlich's behaviours. Mathematical expressions of the equations are as follows [21]:

$$Q_e = \frac{Q_{max} \times K \times C_e}{1 + K \times C_e} \quad (3)$$

$$Q_e = K C_e^{1/n} \quad (4)$$

$$Q_e = \frac{Q_{max} \times (K \times C_e)^n}{1 + (K \times C_e)^n} \quad (5)$$

Where C_e is the equilibrium concentration of solute in solution (mg/L); Q_e is the amount of solute adsorbed per unit mass adsorbent (mg/g); Q_{max} is monolayer adsorption capacity, (mg/g); b is the

constant related the free energy of adsorption; K is the constant indicative of the relative capacity of the adsorbent, (L/g); 1/n is a constant indicative of the intensity of the adsorption.

The isotherms for adsorption of pharmaceutical pollutants by the materials DMDDA-41/A and DMDDA-41/B are shown in Figs 11 and 12.

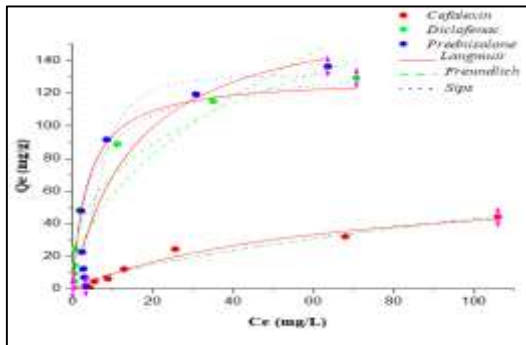


Figure 11. Adsorption isotherms of Cefalexin, Diclofenac and Prednisolone on MCM-41/DMDDA-A

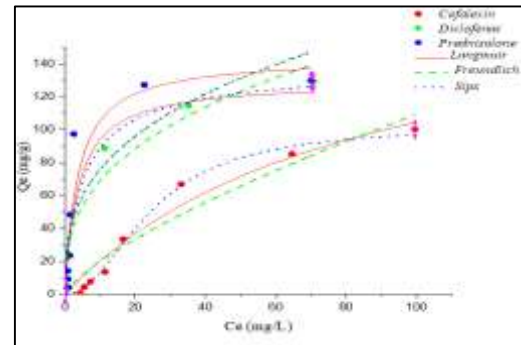


Figure 12. Adsorption isotherms of Cefalexin, Diclofenac and Prednisolone on MCM-41/DMDDA-B

Using the classification of adsorption isotherms, those obtained are of type L "Langmuir". This type is characterized by a decreasing slope as the equilibrium concentration increases, due to the decrease in the number of adsorption sites, following the gradual covering of the surface of the various materials. In this type of adsorption, there is no interaction between the adsorbed molecules: this is a physisorption [22, 44 -52].

the three pharmaceutical pollutants by DMDDA-41/B ($R^2 > 0.97$) and by the Langmuir model in the fixation of the same pollutants by DMDDA-41/A ($R^2 > 0.95$).

The representation of the adsorption isotherms is markedly better by the Sips model in the fixation of

The study of the linearizations of the Langmuir, Freundlich and Sips models (Langmuir-Freundlich), defined above, gives the various parameters of the three models that we have gathered in Table 3.

Table 2. Parameters of the two kinetic models applied to the removal of the three organic pollutants

Materials	Drug	Pseudo 1 st ordre			Pseudo 2 nd ordre		
		k_1 (min^{-1})	Q_e (mg/g)	R^2	k_2 ($g.min^{-1}.mg^{-1}$)	Q_e (mg/g)	R^2
DMDDA-41/A	Céfaléxine	0.002	13,704	0,218	0,001	35,701	0,987
	Diclofénaç	0.003	11,64	0,680	0,002	114,942	0,999
	Prednisolone	0.002	17,884	0,230	0,112	8,992	0,994
DMDDA-41/B	Céfaléxine	0.004	12,591	0,904	0,002	37,537	0,998
	Diclofénaç	0.007	23,757	0,805	0,002	101,214	0,999
	prednisolone	0.003	6,908	0,269	0,021	90,252	0,999

Table 3. Parameters of the adsorption isotherms applied to the removal of the three organic pollutants

Materials	Drug	Langmuir			Freundlich			Sips			
		Q_{max} (mg/g)	K_L (L/g)	R^2	K_F (L/g)	$1/n$	R^2	Q_{max} (mg/g)	K_S (L/g)	n	R^2
DMDDA-41/A	Céfalexine	68,065	0,015	0,965	2,073	0,015	0,937	43,312	0,008	1,430	0,956
	Diclofénaç	127,771	0,262	0,979	30,153	0,360	0,928	140,190	0,246	0,849	0,978
	Prednisolone	176,024	0,062	0,817	17,454	0,516	0,750	131,823	0,014	2,240	0,833
DMDDA-41/B	Céfalexine	193,539	0,011	0,958	3,731	0,733	0,917	102,639	0,001	2,062	0,992
	Diclofénaç	129,771	0,262	0,979	30,153	0,360	0,928	140,190	0,246	0,849	0,978
	prednisolone	144,332	0,272	0,853	34,691	0,340	0,673	128,679	0,104	3,797	0,982

IV . Conclusion

The characterizations show that the parent material obtained is stable and the modification of this material by the addition of amines has not altered its basic structure: the porous diameter and the specific surface area of the materials (amine and deaminated) are greater than those of the parent material, infrared spectroscopy confirms the incorporation of the NH_2 amine groups and thermal analysis proves the resistance of the prepared materials.

The deaminated material has a high binding capacity of Diclofenac ($Q_e=140.190\text{mg/g}$), Prednisolone ($Q_e= 144.332 \text{ mg/g}$), and Cefalexin ($Q_e = 193.539 \text{ mg/g}$). Also, the amino material presents important values in the fixation of the selected pollutants.

For the three pharmaceutical pollutants, the adsorption perfectly follows the pseudo-second order model than the first order one, with $R^2 = 0.99$. The representation of the adsorption isotherms of the two materials, DMDDA-41/A and DMDDA-41/B, is significantly better by the Langmuir model in the case of Diclofenac and Cefalexin, and by the Sips model for Prednisolone. Also, adsorption of the micropollutant is more effective at low concentrations.

Based on the results of the effects studied, the DMDDA functionalized materials give many perspectives in the study of pharmaceutical pollutants. With these results, we can:

- Demonstrate which of the different synthesized materials will have a significant absorption capacity on a wide variety of pharmaceutical pollutants and that this capacity is better in complex solutions.
- Assume that the chosen material can provide an effective solution for the treatment of wastewater treatment plant effluents.
- Contribute to the development of existing wastewater treatment techniques and their performance, in particular in the treatment of effluents containing organic pollutants of pharmaceutical or cosmetic origin.
- Exploit other opportunities to improve the biodegradability of pharmaceutical residues, including biological processes.

V .Acknowledgments

Special thank's to all members of the Chemistry of Materials Laboratory of the University of Oran 1 "LCM" specially Miss Rachida HAMACHA, and the team of Unidad de apoyo a la investigación and Instituto de catálisis y petroleoquímica de Madrid (Spain) for their valuable support, encouragement and collaboration.

VI. References

1. Chiola, V.; Ritsko, J. E.; Van der Pool, C. D. Process for producing low-bulk density silica U. S. *Patent Office* 3 (1971) 556-725.
2. Beck, J.S.; Vartuli, J.C.; Roth, W.J.; Leonowicz, M.E.; Kresge, C.T.; Schmitt, K.D.; Chu, C. T.W.; Olson, D.H.; Sheppard, E. A new family of mesoporous molecular sieves prepared with liquid crystal templates. *Journal of the American Chemical Society* 114 (1992) 108, 340.
3. Zhao, X.S.; Lu, G.Q.M.; Millar, G.J. Advances in Mesoporous Molecular Sieve MCM- 41. *Industrial & Engineering Chemistry Research* 35 (7) (1996).
4. Kresge, C.T.; Leonowicz, M.E.; Roth, J.W.; Vartuli, J.C.; Beck, J.S. Ordered mesoporous molecular sieves synthesized by a liquid-crystal template mechanism. *Nature*, 359 (1992) 710-712.
5. Hickey, A.J.; Smyth, H.D.C. Pharmaco-Complexity, Outlines in Pharmaceutical Sciences. *American Association of Pharmaceutical Scientists* 2011.
6. Jishuai, B.; Chun, H.; Yulun, N.; Min, Y.; Jiuhui, Q. Mechanism of Catalytic Ozonation in $Fe_2O_3/Al_2O_3@SBA-15$ Aqueous Suspension for Destruction of Ibuprofen. *Environnemental. Sciences Technology* (2015) 1-32.
7. McCusker, L.B.; Liebau, F.; Engelhardt, G. Microporous and Materials. *Pure Applied Chemistry* 73 (2001) 381-394 .
8. Wang, X.; Lin, K.S.K.; Sheng, J.C.C. Direct Synthesis and Catalytic Applications of Ordered Large Pore Aminopropyl-Functionalized SBA-15 Mesoporous Materials. *Journal of Physical Chemistry B* 109 (2005) 1763-1769.
9. Zhang, Y.; Wang, H.; Gao, C.; Li, X.; Li, L. Highly ordered mesoporous carbon nanomatrix as a new approach to improve the oral absorption of the water-insoluble drug, simvastatin. *European Journal of Pharmaceutical Sciences* 49 (2013) 864-872.
10. Rashi, S.; Prajapati, S.K.; Singh, D. Mesoporous Silica Nanoparticles for Controlled Drug Delivery. *World Journal of Pharmacy and Pharmaceutical Sciences* 4 (6) (2013) 332-347.
11. Enrique, V.G.; Cecilia, J.A.; Moya, E.M.O; Jr Celio, L.C.; Diana, C.S.A; Enrique, R.C. Low Cost Pore Expanded SBA-15 Functionalized with Amine

- Groups Applied to CO₂ Adsorption. *Materials* 8 (2015) 2495-2513.
12. Claudio, A.V.; Oliveira, V. Hydrophobic contribution to amoxicillin release associated with organofunctionalized mesoporous SBA-16 carriers. *Materials Research Bulletin* 7522 (2014) 1-35.
 13. Javad, S.; Zohre, Z. Advanced drug delivery systems: Nanotechnology of health design A review. *Journal of Saudi Chemical Society* 18 (2013) 85–99.
 14. Marie, H.J. Medicaments et environnement. *Académie nationale de Pharmacie* (2008), Paris, France.
 15. Staub, P.F. Les substances émergentes dans l'environnement. *Office National de l'Eau et des Milieux Aquatiques (ONEMA)* (2009), Paris, France.
 16. Melissa, B. Impacts des substances pharmaceutiques sur l'eau et les milieux aquatiques. *Office International de l'Eau (OIEau)* (2010), Paris, France.
 17. Loos, R.; Locoro, G.; Comero, S.; Contini, S.; Schwesig, D.; Werres, F.; Balsaa, P.; Gans, O.; Weiss, S.; Blaha, L.; Bolchi, M.; Gawlik B.M. Pan-European survey on the occurrence of selected polar organic persistent pollutants in ground water. *Water Research* 44 (2010) 4115-4126.
 18. Loos, R.; Gawlik, B.M.; Locoro, G.; Rimaviciute, E.; Contini, S.; Bidoglio, G. EU-wide survey of polar organic persistent pollutants in European river waters. *Environmental Pollution* 157 (2009) 561–568.
 19. Wantala, K.; Sthiannopkao, S.; Srinameb, B.; Grisdanurak, N.; Kim, K.W. Synthesis and characterization of Fe-MCM-41 from rice husk silica by hydrothermal technique for arsenate adsorption. *Environmental Geochemistry and Health* 32(4) (2010) 261–266.
 20. Hermida, L.; Abdullah, A.Z.; Mohamed, A.R. Effects of functionalization conditions of sulfonic acid grafted SBA-15 on catalytic activity in the esterification of glycerol to monoglyceride: a factorial design approach. *Journal of Porous Materials* 19 (5) (2012) 835–846.
 21. Dubois, M.; Gulik-Krzywicki, T.; Cabane, B. Growth of silica polymers in a lamellar mesophase. *Langmuir* 9 (3) (1993) 673-680.
 22. Barczak, M.; Wierzbicka, M.; Borowski, P. Sorption of diclofenac onto functionalized mesoporous silicas: Experimental and theoretical investigations. *Microporous and Mesoporous Materials* 264 (2018) 254-264.
 23. Nassi, M.; Sarti, E.; Pasti, L.; Martucci, A.; Marchetti, N.; Cavazzini, A.; Galarneau, A. Removal of perfluorooctanoic acid from water by adsorption on high surface area mesoporous materials. *Journal of Porous Materials* 21 (4) (2014) 423–432.
 24. Suriyanon, N.; Punyapalaku, P.; Ngamcharussrivichai, C. Mechanistic study of diclofenac and carbamazepine adsorption on functionalized silica-based porous materials. *Chemical Engineering Journal* 214 (2013) 208–218.
 25. Carniti, P.; Gervasini, A. Liquid-Solid Adsorption Properties: Measurement of the Effective Surface Acidity of Solid Catalysts. *Calorimetry and Thermal Methods in Catalysis* 154 (2013) 543-551.
 26. Krasucka, P.; Goworek J. MCM-41 silica as a host material for controlled drug delivery systems. *Annales Universitatis Mariae Curie-Skłodowska, sectio AA – Chemia* 70 (2) (2015) 45.
 27. Loos, R.; Carvalho, R.; Antonio, D.C.; Comero, S.; Locoro, G.; Tavazzi, S.; Paracchini, B.; Ghiani, M.; Lettieri, T.; Blaha, L.; Jarosova, B.; Voorspoels, S.; Servaes, K.; Haglund, P.; Fick, J.; Lindberg, R.H.; Schwesig, D.; Gawlik, B.M. EU-wide monitoring survey on emerging polar organic contaminants in wastewater treatment plant effluents. *Water Research* 47 (2013) 6475-6487.
 28. Dahanea, S.; Galeraa, M.M.; Marchionna, M.E.; Viciana, M.M.S.; Derdour, A.; García, M.D.G. Mesoporous silica based MCM-41 as solid-phase extraction sorbent combined with micro-liquid chromatography-quadrupole-mass spectrometry for the analysis of pharmaceuticals in waters. *Edition Talanta* 152 (2016) 378-391.
 29. Benhamou, A.; Baudu, M.; Derriche, Z.; Basly, J.P. Aqueous heavy metals removal on amine-functionalized Si-MCM-41 and Si-MCM-48. *Journal Hazard Mater* 171 (2009) 1001–1008.
 30. Engineering Techniques, Measurement-Analyses, Analytical Techniques, Thermal Methods of Analysis «article updated from P 1260 published in 2001».
 31. Showkat, A.M.; Zhang, Y.P.; Kim, M.S.; Lyenger, A.; Karla, G.; Reddy, R.A.; Lee, K.P. Analysis of Heavy Metal Toxic Ions by Adsorption onto Amino-functionalized ordered Mesoporous Silica. *Bull. Kor. Chemical Society* 28 (2007) 1985-1992.
 32. Dada, A.O.I.; Olalekan, A.P.; Olatunya, A.M. Langmuir, Freundlich, Temkin and Dubinin–Radushkevich Isotherms Studies of Equilibrium Sorption of Zn²⁺ Unto Phosphoric Acid Modified Rice Husk. *IOSR Journal of Applied Chemistry (IOSRJAC)* 3 (1) (2012) 38-45.
 33. Brunauer, S.; Emmett, P.H.; Teller, E. Adsorption of Gases in Multimolecular Layers. *Journal of the American Chemical Society* 60 (1938) 309 – 319.
 34. Ariapad, A.; Zanjanchi, M.A.; Arvand, M. Efficient removal of anionic surfactant using partial template-containing MCM-41. *Desalination* 284 (2012) 142–149.
 35. Morsli, A.; Benhamou, A.; Basly, J.P.; Baudu, M.; Derriche, Z. Mesoporous silicas: improving the adsorption efficiency of phenolic compounds by the removal of the amino group from functionalized silicas. *Journal Royal Society of Chemistry (RSC) Advances* 5 (2015) 41631-41638.
 36. Idris, S.A.; Alotaibi, K.M.; Peshkur, T.A.; Anderson, P.; Morris M.; Gibson, L.T. Adsorption kinetic study: Effect of adsorbent pore size distribution on the rate of Cr (VI) uptake. *Microporous and Mesoporous Materials* 165 (2013) 99–105.
 37. Benhamou, A.; Basly, J.P.; Baudu, M.; Derriche, Z.; Hamacha, R. Amino-functionalized MCM-41 and MCM-48 for the removal of chromate and arsenate. *Journal of Colloid and Interface Science* 404 (2013) 135–139.
 38. Trindade, F.J.; Rey, J.F.Q.; Brochsztain, S. Modification of molecular sieves MCM-41 and SBA-15 with covalently grafted pyromellitimide and 1,4,5,8-naphthalenediimide. *Journal of Colloid and Interface Science* 368 (2012) 34–40.
 39. Yokoi, T.; Kubota, Y.; Tatsumi, T. Amino-functionalized mesoporous silica as base catalyst and adsorbent. *Applied Catalysis A: General* 421-422 (2012) 14–37.
 40. CHEN, J. P.; WANG L. Characterization of metal adsorption kinetic properties in batch and fixed-bed reactors. *Chemosphere* 54 (3) (2004) 397-404.
 41. Da'na, E. Adsorption of heavy metals on functionalized-mesoporous silica: A review. *Microporous and Mesoporous Materials* 247 (2017) 145-157.
 42. Li, G.; Wang, B.; Sun, Q.; Xu, W.; Han, Y. Adsorption of lead ion on amino-functionalized fly-ash-based SBA-15 mesoporous molecular sieves prepared via two-step hydrothermal method.

- Microporous and Mesoporous Materials* 252 (2017)
43. Boukoussa, B.; Kibou, Z.; Abid, Z.; Ouargli, R.; Braham, N.C.; Villemain, D.; Hamacha, R. Key factor affecting the basicity of mesoporous silicas MCM-41: effect of surfactant extraction time and Si/Al ratio. *Chemical Papers* 72 (2) (2017) 289–299.
 44. Albayati, T.M.; Jassam, A.A.A. Experimental Study of Drug Delivery system for Prednisolone Loaded and Released by Mesoporous Silica MCM-41. *Al-Khwarizmi Engineering Journal* 15 (1) (2019) 117-124.
 45. Albayati, T.M.; Jassam, A.A.A. Synthesis and characterization of mesoporous materials as a carrier and release of prednisolone in drug delivery system. *Journal of Drug Delivery Science and Technology* 53 (2019) 101-176.
 46. Maria, G.; Stoica, A.I.; Luta, I.; Stirbet, D.; Radu, G.L. Cephalosporin release from functionalized MCM-41 supports interpreted by various models. *Microporous and Mesoporous Materials* 162 (2012) 80–90.
 47. Uthappa, U.T.; Brahmkhatri, V.; Sriram, G.; Jung, H.Y.; Yu, J.; Kurkuri, N.; Aminabhavi, T.M.; Altalhi, T.; Neelgund, G.M.; Kurkuri, M.D. Nature engineered diatom biosilica as drug delivery systems. *Journal of Controlled Release* 281 (2018) 70-83.
 48. Alivand, M.S.; Najmi, M.; Tehran, N.H.M.H.; Kamali, A.; Tavakoli O.; Rashid, A.; Esrafil, M.D; 105-115.
 49. Ghasemy, I.; Mazaheri O. Tuning the surface chemistry and porosity of waste-derived nanoporous materials toward exceptional performance in antibiotic adsorption: Experimental and DFT studies. *Chemical Engineering Journal* 374 (2019) 274-291
 50. Nairi, V.; Medda, L.; Monduzzi, M.; Salis, A. Adsorption and release of ampicillin antibiotic from ordered mesoporous silica. *Journal of Colloid and Interface Science* 497 (2017) 217–225.
 51. Wolfe, D.; Schorr, M.; Hanson, M.; Nelson, C.H.; Richards, S.M. Hazard assessment for a pharmaceutical mixture detected in the upper Tennessee River using *Daphnia magna*. *Global Journal of Environmental Science and Management* 1 (2015)1-14.
 52. Moritz, G.M.; Moritz, M. APTES-modified mesoporous silicas as the carriers for poorly water-soluble drug. Modeling of diflunisal adsorption and release. *Applied Surface Science* 368 (2016) 348–359.
 53. Hebig, K.H.; Groza, L.G.; Sabourin, M.J.; Scheytt, T.J.; Ptacek, C.J. Transport behavior of the pharmaceutical compounds carbamazepine, sulfamethoxazole, gemfibrozil, ibuprofen, and naproxen, and the lifestyle drug caffeine, in saturated laboratory columns. *Science of The Total Environment* (590–591) (2017) 708-719.

Please cite this Article as:

Benyoub N., Benhamou A., Debab. A., Amino functionalized mesoporous silica for drug adsorption. *Algerian J. Env. Sc. Technology*, 8:4 (2022) 2772-2781